LUPINE PUBLISHERS

Modern Approaches on Material Science

DOI: 10.32474/MAMS.2023.05.000216

ISSN: 2641-6921

Research Article

A Novel Method with Thermal and Press Coupling Effect to Prepare Fe-Based Amorphous Alloy Coatings

Weiwei Dong[1,2], Danbo Qian[1], Minshuai Dong[1], Jiankang Zhang[1], Zixiao Wang[1] and Shigen Zhu[1,2]*

[1]*College of Mechanical Engineering, Donghua University, China*

[2]*Engineering Research Center of Advanced Textile Machinery, Ministry of Education, China*

***Corresponding author:** Shigen Zhu, College of Mechanical Engineering, Donghua University, Shanghai 201620, PR China

Received: September 12, 2023 **Published:** September 19, 2023

Abstract

A novel method with thermal and press coupling effect is proposed for producing Fe-based amorphous alloy coating. The dense Fe-based amorphous alloy coating could be fabricated without any porosity or cracks, and the thickness of Fe-based amorphous alloy coating is about 25μm. The content of amorphous phase in coating is about 70%. The metallurgical joint between substrate and coating could be achieved. The hardness of coating is up to 974HV, which increased by 322% compared with the substrate. At the same condition, the worn rate of the coating is 31mg, which decreased by 71% compared with the substrate. The improvement of hardness and wear resistance is attributed to the maintained amorphous phase and precipitated nano α-Fe (Si) in the coating.

Keywords: Amorphous Alloy; Coating; Electrical Contact Strengthening; Hardness; Wear Resistance

Introduction

Fe-based amorphous alloy shows ultra-high-strength and hardness, excellent wear and corrosion resistance, superior soft magnetic properties and low economic cost, and is expected to be a key structural material in aerospace equipment, biomedical devices, precision equipment, and other fields. Thermal spray and cladding techniques have been used to prepare amorphous alloy coating. Mostly, the amorphous alloy powders are selected as the row materials. In the thermal spraying process, the amorphous alloy powders are sprayed onto the substrate's surface in a semi-molten state, deformed plastically, and stacked to the coating [1-3]. In the conventional cladding process, the particles would go through the melting re-solidification process [4-6]. The oxidation, crystallization, layered structure of coating are inevitable in this traditional technology, which would be detrimental to properties and bond strength between coating and substrate. The amorphous coating fabricated by classical thermal spraying usually has low adhesion strength and high porosity (2%–5%) [7-9]. The coatings fabricated by a conventional laser cladding have a low content of amorphous phase, which can easily induce brittle cracks due to the high heat input and dilution ratio [10-12]. Unlike traditional thermal spraying and cladding technology, the self-developed electric contract strength technology (ECS) is a new high-efficient coating preparative technology [13-15]. In this paper, the ECS technology and Fe-based amorphous ribbons are used to fabricate amorphous alloy coating, and the content of the amorphous phase, hardness, worn rate and worn surface are studied in this work.

The principle of electric contract strength process

The schematic diagram is shown in (Figure 1). According to the "Joule-Lenz law", a large amount of Joule heat will be produced at the interface when the current pass through the workpiece, coating and their interface. With the temperature increases, the corresponding area next to the interface could be softening, and atomic activity could be increasing. Under the pressure of the electrode wheel,

plastic deformation of workpiece surface and coating, melting and atomic diffusion at the interface would proceed simultaneously. The metallurgical joint between coating and matrix can be achieved. Then the contact resistance between workpiece and coating decreases rapidly, and so does the heat production of the coating system. With the rotation of the electrode wheel, temperature of the coating decreases rapidly. The amorphous alloy coating has undergone a rapid heating and cooling process. Meanwhile a small number of crystals will precipitate in the amorphous matrix.

Due to the short pulse time of current (only 0.02s) and less heat dissipation, the total heat Q is obtained from Formula 1-1 [16,17].

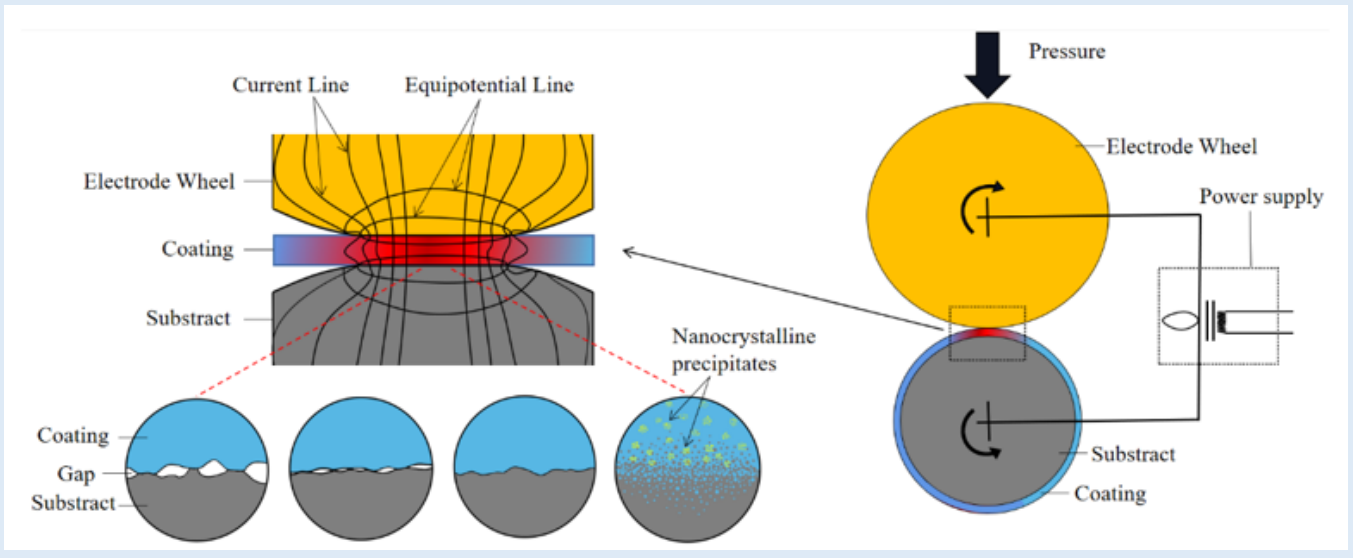

Figure 1: The schematic diagram of electric contract strength process

Where, i is the dynamic value of the current intensity through the contact area, r_{cw} is the dynamic value of the contact resistance between the workpiece and electrode, r_w is the dynamic value of the internal resistance of the workpiece and coating, and t is the conduction time.

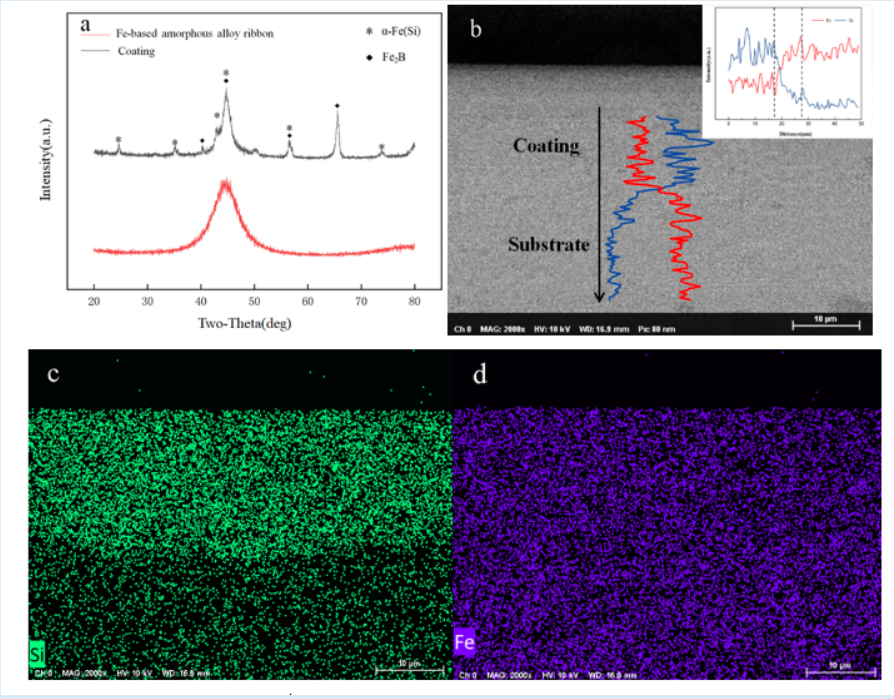

Figure 2: XRD patterns of Fe-based amorphous alloy ribbon and the fabricated coating (a), SEM image and elemental analysis of Fe-based amorphous alloy coating(b-d)
Figure 2b: d shows the typical morphology SEM images and elemental analysis of Fe-based alloy coating

Where, α is the resistance temperature coefficient, r_{w0} is the resistivity of the material at T=0℃, T is the temperature.

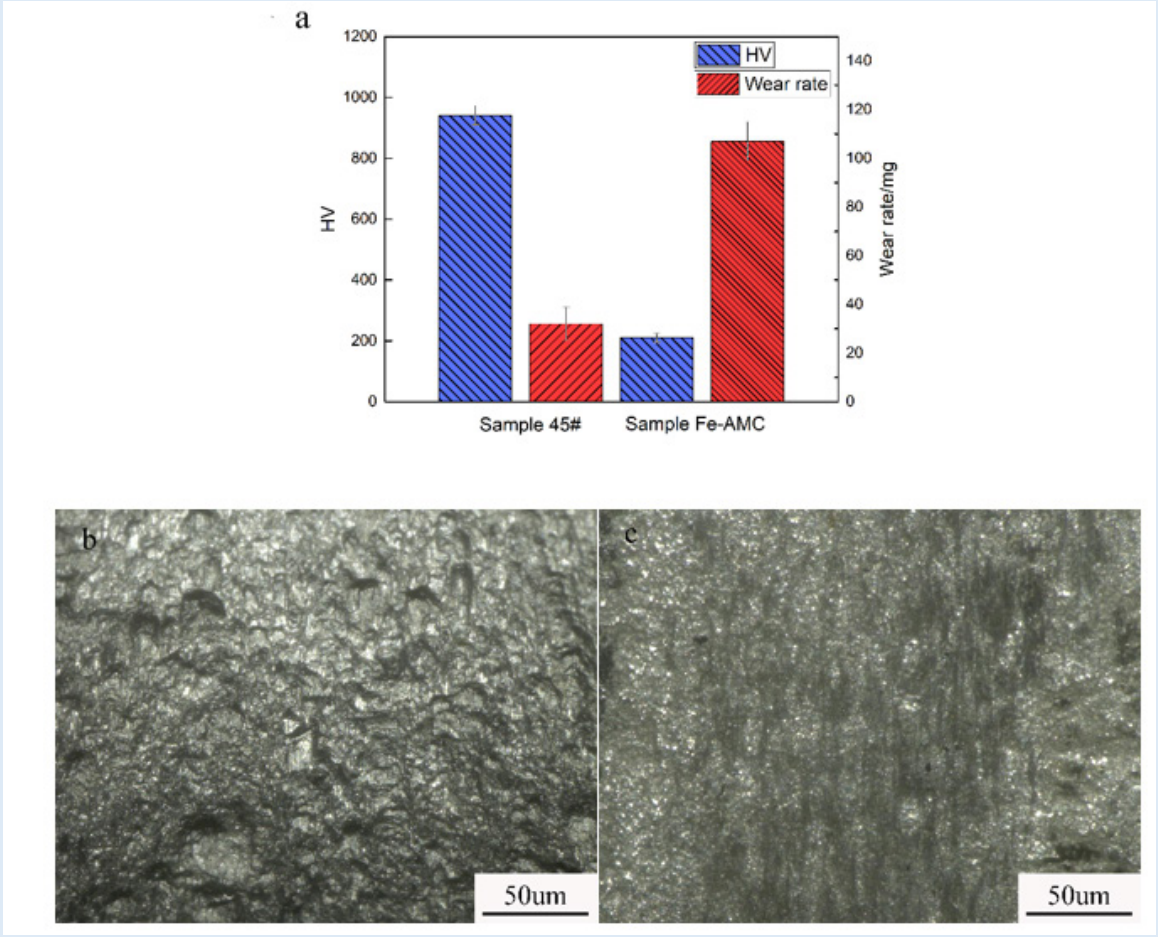

Figure 3: the hardness, wear rate(a) and worn surface of 45# steel with or without Fe-based amorphous alloy coating (b, c)

Where, ρ is the equivalent resistivity, σ_s is the mean square error of the height of the rough peak on the rough surface, and F is the contact pressure.

Compared with the existing thermal spray and cladding techniques, the ECS technology for fabricating amorphous alloy coating has the following advantages:

a) The Fe-based amorphous alloy ribbon is selected as raw material to prepare coating, there is no powder densification during the coating forming process, which results in the simplification of coating forming process. The quality of coating can be controlled.

b) Joule heat act as inner heat source. The maximum heat is generated at the interface. With the combined action of pressure, the metallurgical joint could be achieved at lower temperature, and stratification could be avoided.

c) During the ECS process, the amorphous alloy ribbons didn't melt, little oxidation would occur.

d) With the combined action of pressure, the ECS technology shows high usage rate of material and heat.

Experimental

The as-cast $Fe_{78}Si_9B_{13}$ amorphous alloy ribbons with a thickness of 25±2μm was used in this study to fabricate the Fe based coatings. The normalized 45# steel ring specimen with the dimensions of φ168 mm × φ150 mm × 50 mm was selected as the substrate. The novel technology named electrical contact strengthening (ECS) was used to fabricate the coating on the substrate. Here, the electric current of 20kA, contact pressure of 2.0 kN, rotating speed of 0.5 r/min, electrode speed of 0.2 mm/min were employed to prepared coating in this study. The microstructure was examined by field emission scanning electron microscopy (FESEM) with energy dispersive spectroscopy (EDS). The phases were identified by X-ray diffraction (XRD). The hardness was measured by HXS-1000A type hardness tester. The wear test was carried out according to standard ASTM G77 [18-25].

Results and Discussion

Microstructure and phase constitution

Figure 2a presents the X-ray diffraction patterns of Fe-based amorphous alloy ribbons and the fabricated coating (Fe-AMC). The XRD pattern of alloy ribbons show a broad diffraction halo, suggesting a typical amorphous structure, while the XRD pattern of coating exhibit several crystalline diffraction peak which are shown to be α-Fe (Si) solid solution, Fe_2B. The volume percent of amorphous phase in the coatings was calculated up to 70% by Pseudo-Voigt function fitting with the method of Verdon, meaning the coating mainly consisted of amorphous structure. alloy coating. It can be seen that the interface between the coating and substrate is not clear. From the SEM-EDS mappings of Fe and Si elements (Figure 2c-d). It can be confirmed that the thickness of the coating is about 25 μm approximately, which is consist with the raw amorphous alloy ribbon. From the EDS line scanning (Figure 2b). It also can be found that a distinct transition zone at interfaces between coating and substrate, which wide is about 10μm. From the cross-sectional morphology, it can be seen that the coating is well bonded on the substrate without no obvious cracks or pores. The metallurgical joint and dense structure of coating fabricated by ECS is well different from that prepared by thermal spray and cladding techniques which is attribute to the distinctive character -rapid heating and pressure coupling effect. Meanwhile, with the coupling work of the pressure, the Fe-base alloy ribbons become rapidly soft or local melting, and the atoms diffuse quickly through the interface. Little nano-α-Fe (Si), Fe_2B phase would precipitate in the amorphous alloy matrix [26-30].

Hardness and wear resistance

The hardness of substrate (45#) and Fe-AMC is shown in Figure 3a. It can be seen that the average hardness of the coatings is about 974HV, which is significantly higher than 230HV of the substrate. The ultra-hardness of the Fe-based amorphous alloy coating comes from the maintain of the amorphous phase and the distribution of nanoscale Fe_2B and α-Fe (Si). The worn rate of the sample 45# is 102 mg, while the worn rate of sample Fe-AMC is 31mg which is less than that for the 45# steel samples. The worn surfaces of samples 45# and sample Fe-AMC are shown in Figure 3(b-c). There are many pits on the worn surfaces of samples 45#. The surface failure subjected to the alternative shearing force and compressive stress, causing plastic deformation, fatigue crack and local peeling on the surface. Besides, there are little pit on the worn surface of sample Fe-AMC. It could be induced that the wear mode of Fe-based amorphous alloy coating has changed. It is attributed to the higher hardness of the coating, uniform distribution of the nano α-Fe (Si) phase and FeB_2 particles in the coatings and high coating bond strength [31-33].

Conclusion

The Fe-based amorphous alloy coating could be fabricated by electric contact strength technology without any porosity or cracks. The thickness of coating with a high amorphous content is about 25mm. The volume fraction of amorphous phase in coating could be 70% approximately. The interface between substrate and Fe-based amorphous alloy ribbons is metallurgical joint. The hardness of coating up to 974HV, which increased by 322% as compared with the substrate. At the same wear condition, the wear rate of the coating is 31mg, which decreased by 71% compared with the substrate.

Author contributions

The manuscript was written through contributions of all authors. All authors have given approval to the final version of the manuscript.

Declaration of Competing Interest

The authors declare that they have no known competing financial interests or personal relationships that could have appeared to influence the work reported in this paper.

Acknowledgments

This work was supported by Chinese Universities Scientific Fund (23D110306).

References

1. Han C, Ma L, Sui X Ma X, Huang G (2021) Coatings 11 695.
2. Sun YJ, Yang R, Xie L, Wang SL (2022) Surf Coat Tech 436: 128316.
3. https://doi.org/10.1016/j.surfcoat.2022.128316.
4. Lee CY, Lin TJ, Sheu HH, Lee J (2021) Mater Res Technol 15: 4880-4895.
5. https://doi.org/10.1016/j.jmrt.2021.10.103.
6. Xiao H. Gao L, Sun Z, Wang G, Jiang Q, et al. (2021) Mater Lett 297. 130002.
7. https://doi.org/10.1016/j.matlet.2021.130002.
8. Chen H, Cui H, Jiang D, Song X, Zhang G, et al. (2022) J Alloy Compd 899:163277.
9. https://doi.org/10.1016/j.jallcom.2021.163277.
10. Wang HZ, Cheng YH, Yang JY, Wang QQ (2020) J Non-Cryst Solids 550.120351.
11. https://doi.org/10.1016/j.jnoncrysol.2020.120351.
12. Zhang S, Wang X, Yang S, Hao Y, Chen H, et al. (2021) Surf Coat Tech 425.127659,
13. https://doi.org/10.1016/j.surfcoat.2021.127659.
14. Zhou Z, Zhang Y, Chen X, Liang B (2021) Surf Coat Tech 408. 126800.
15. https://doi.org/10.1016/j.surfcoat.2020
16. Guo SF, Pan HJ, Zhang DF, Zhang JF, Wang J, et al. (2016) Mater Design 108: 624-631.
17. https://doi.org/10.1016/j.matdes.2016.07.031.
18. Su Y, Yue T (2020) Mater Today Commun 25.101715.
19. https://doi.org/10.1016/j.mtcomm.2020.101715.
20. Shu F, Zhang B, Liu T, Sui S, Liu Y, et al. (2019) Surf Coat Tech 358. 667-675,
21. https://doi.org/10.1016/j.surfcoat.2018.10.086.

22. Shu F, Tian Z, Zhao H, He W, Sui S, et al. (2016) Mater Lett 176. 306-309
23. https://doi.org/10.1016/j.matlet.2016.04.118.
24. Sun Z, Zhu SG, Dong WW, Bai YF, et al. (2021) Surf Coat Tech 421: 127289.
25. https://doi.org/10.1016/j.surfcoat.2021.127289.
26. Xu MK, Zhu SG, Ding H, Qi QB (2022) Int J Refract Met H 62: 70-77.
27. https://doi.org/10.1016/j.ijrmhm.2016.10.017.
28. Qi, Zhu SG (2015) Appl Surf Sci 349: 792-797.
29. https://doi.org/10.1016/j.apsusc.2015.05.064.
30. Greenwood JH (1966) Tripp, Journal of Applied Mechanics.
31. https://doi.org/10.1115/1.3607616.
32. Greenwood JA (1966) Brit.J. App l. Phys 17:1621-1632.
33. https://iopscience.iop.org/article/10.1088/0508-3443/17/12/310/meta.

DOI: 10.32474/MAMS.2023.05.000216